Journal of Applied Pharmaceutical Research
Volume 14 Issue 4, Year of Publication 2026, Page 210 – 223
DOI: https://doi.org/10.69857/joapr.v14i4.1973

Check for updates

Research Article

JOURNAL OF APPLIED PHARMACEUTICAL RESEARCH | JOAPR
www.japtronline.com *ISSN: 2348 – 0335*

FORMULATION AND EVALUATION OF FACTORIAL DESIGN BASED SULFASALAZINE-LOADED ETHOSOMAL GEL FOR RHEUMATOID ARTHRITIS

Sanjaikumar D*, Anasuya Patil, Hemanth G

Article Information
Received: 5th March 2026
Revised: 20th June 2026
Accepted: 7th July 2026
Published: 31st July 2026

Keywords
Sulfasalazine, Rheumatoid Arthritis, Ethosomes, Full Factorial Design, Transdermal Delivery, Anti-inflammatory Activity.

ABSTRACT

Background: Oral administration of sulfasalazine for rheumatoid arthritis is associated with limitations that reduce therapeutic effectiveness. Transdermal delivery using ethosomal vesicles offers a promising strategy to enhance skin penetration and provide localized therapeutic effects. **Methodology:** Sulfasalazine-loaded ethosomes were formulated using the cold method and optimized using a 3^2 full factorial design across nine experimental trials. The formulations were characterized for vesicle size, polydispersity index (PDI), zeta potential, entrapment efficiency, and morphology using atomic force microscopy (AFM). The optimized ethosomal formulation was incorporated into a 1% Carbopol 934 gel to prepare the ethosomal gel (EGL). Ex vivo permeation studies were performed using rat skin to compare EGL with a conventional gel (CGL), and flux and permeability coefficients were calculated. Anti-inflammatory activity was assessed in Sprague–Dawley rats. **Results and Discussion:** Particle sizes ranged from 98.3 ± 2.37 nm to 187.7 ± 3.12 nm, with a negative zeta potential ranging between –24.2 ± 2.56 mV and –32.6 ± 1.35 mV. The entrapment efficiency ranged from 85.33 ± 3.84% to 94.62 ± 1.34%. Vesicles displayed smooth and spherical surfaces. In vitro drug release studies of the ethosomal gel formulations lasted 12 hours, revealing controlled release of sulfasalazine and enhanced ex vivo permeation in the optimized formulation. In vivo studies showed that EGL produced a greater reduction in inflammation compared to CGL. **Conclusion:** The developed ethosomal gel demonstrated enhanced skin permeation and anti-inflammatory efficacy, making it a promising transdermal delivery system for sulfasalazine in the management of rheumatoid arthritis.

INTRODUCTION

An autoimmune condition called rheumatoid arthritis affects about 1% of people in India. This frequent inflammatory condition of unknown etiology is characterized by inflammation of the synovial membrane, leading to joint swelling and thickening of the membrane due to increased synovial exudate [1,2]. Morbidity and shortened life spans were the outcomes of the illness. In the early phases of the disease, immune complexes and autoantibodies were the main focus; however, later research revealed that rheumatoid synovial membrane tumor-like behavior and T-cell-independent cytokine networks are associated with the disease [3,4].

*Department of Pharmaceutics, KLE College of Pharmacy, Rajajinagar, Bengaluru– 560010, Karnataka, India.

***For Correspondence:** **sanjaidurai20@gmail.com**

Sulfasalazine (SSZ) is a sulfonamide drug that contains sulfapyridine and 5-aminosalicylic acid. It may also be referred to as 2-hydroxy-5-[[4-(pyridin-2-ylsulfamoyl) phenyl] diazenyl] benzoic acid and has the molecular formula $C_{18}H_{14}N_4O_5S$. It has demonstrated anti-inflammatory properties, possibly by blocking T cells, the NF-κB pathway, and, in particular, proinflammatory cytokines [5,6]. Rheumatoid arthritis and other inflammatory diseases, including human Crohn's disease, have been treated with it as normal practice [7-11]. In addition to its extensive metabolism, limited water solubility, poor absorption, instability, and poor pharmacokinetic properties, SSZ also has low oral bioavailability [12]. Sulfasalazine, a DMARD, has a half-life of 5-7 h and is used to treat rheumatoid arthritis. Oral use is discouraged for frequent dosing, but vesicle encapsulation enhances targeted delivery, improving patient compliance. Sustained transdermal delivery ensures consistent anti-inflammatory drug levels, overcoming the skin barrier [13,14].

Topical drug delivery systems facilitate the delivery of drugs to the skin's surface for the treatment of inflammatory and other skin conditions. The drug undergoes first-pass metabolism in the topical delivery mechanism. However, getting a drug through the stratum corneum barrier is one of the major challenges with the topical drug delivery system [15,16]. Numerous methods, including sonophoresis and iontophoresis, have been studied to enhance drug penetration into the skin. Similarly, lipid-based vesicular systems such as liposomes, ethosomes, niosomes & transferosomes exhibit improved permeability [17].

Ethosomes are soft, malleable vesicles composed of ethanol, water, and phospholipids that are used as non-invasive drug delivery systems. Ethosomes range in size from microns to nanometers. They have slightly modified liposomes with a high ethanol concentration that enables them to penetrate through the stratum corneum [18,19]. In addition, the vesicles become softer, more flexible, and more stable at high ethanol concentrations. They provide better bioavailability and distribution of therapeutically active drugs to the deep layers of the skin [20,21].

To deliver the drug topically, these ethosomes are also incorporated into the gel. Gels are colloidal substances comprising tiny inorganic or substantial organic particles dispersed within a liquid medium, designed for topical application on the skin. Gels have the characteristics of solids and are two-phase systems with various forms of continuous structure present. Three-dimensional matrices are formed in hydrophilic liquids by a relatively small amount of either a natural or a synthetic polymer [22].

Although sulfasalazine has poor bioavailability and a short half-life, in vivo pharmacokinetic (PK) evaluation was not included in the present study due to limited access to animal facilities and ethical approvals. The current work focuses on in vitro and ex vivo assessments to establish the permeation-enhancing potential of ethosomal delivery. Future studies involving comprehensive PK profiling in animal models are planned to validate the ethosomal gel's ability to enhance bioavailability.

In the present study, sulfasalazine-loaded ethosomes were prepared, and a 3^2 full factorial design was used to statistically optimize the formulation parameters. To enhance skin retention during transdermal administration, the optimized formulation was mixed with an appropriate 1% Carbopol 934 gel.

MATERIALS AND METHOD

Material

Sulfasalazine & Soya lecithin were obtained from Yarrow Chemicals, Mumbai; Propylene glycol and Carbopol 934 from SD Fine Chem Ltd., Mumbai; Ethanol from Fine Chemicals, Mumbai; Cholesterol from Central Drug House Ltd., New Delhi; and Triethanolamine from Loba Chemie Pvt. Ltd., Mumbai. The dialysis membrane was procured from Hi-Media Pharmaceuticals Pvt. Ltd., and Sprague–Dawley (SD) rats were obtained from Invivo Bioscience. All other chemicals and reagents used were of analytical grade, unless otherwise specified.

Animals

A total of 27 male Sprague–Dawley (SD) rats were obtained from Invivo Bioscience and used in experiments. The experiments were designed in accordance with the guidelines and regulations of the Committee for the Purpose of Control and Supervision of Experiments on Animals (CPCSEA). The Institutional Animal Ethics Committee (IAEC) approved the experimental procedures under IAEC No. Invivo/007/2024. During the 3-day acclimatization period, the rats had unlimited access to food and water and were housed in standard polypropylene cages at a density of 9 rats per cage. The animal housing environment was maintained at an average temperature of 23 °C with a 12-hr light-dark cycle.

Method of preparation

Sulfasalazine-loaded ethosomes were prepared using a well-established cold method. In brief, a mixture of ethanol and propylene glycol was used to dissolve sulfasalazine, SPC, and cholesterol, and in a covered glass beaker, the solution was mixed at 1500 rpm using a magnetic stirrer. The ethanolic solution was stirred for 30 minutes after the addition of distilled water. Finally, the mixture was sonicated using a probe sonicator (Servewell Instruments Pvt. Ltd., India) for 10 min (3 cycles). Following sonication, the sulfasalazine-loaded ethosomes were stored under refrigerated conditions, as shown in Figure 1 [23].

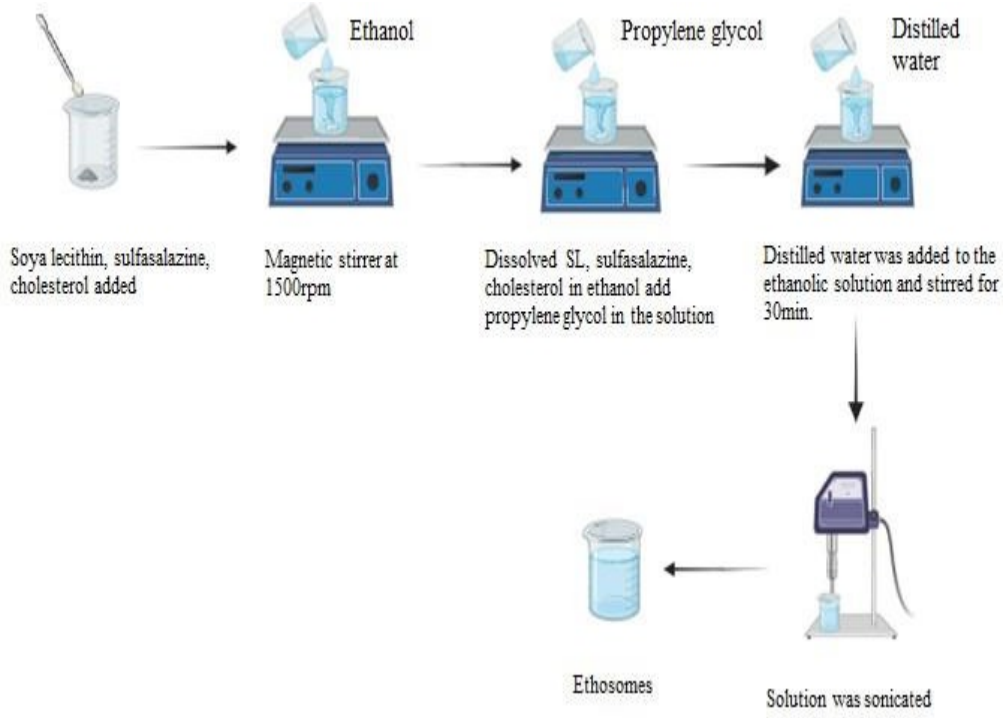

Figure 1: Formulation of ethosomes using a cold method.

Optimization of ethosomal formulation

The optimization of the ethosome formulation strongly influences composition and development strategy. Entrapment efficiency (EE%), vesicle size (nm), and zeta potential (mV) were the dependent variables, and the effects of the selected independent variables, soy lecithin (X_1) and ethanol (X_2), were examined using a 3^2 experimental design. In the factorial design, soy lecithin was evaluated at concentrations of 2%, 3%, and 5% (w/w), while ethanol was studied at 20%, 35%, and 50% (v/v), corresponding to the coded levels -1, 0, and +1, respectively. Preliminary studies were conducted to identify three levels of the independent variables before implementing the experimental design. Constant processing variables and formulation components were used in the optimization process, guided by an experimental design [24]. The summary experimental units, runs, and factor combinations taken into consideration in this investigation were derived from the coded levels in (Table 1) & (Table 2). Statistical analysis of the experimental design was performed using Minitab®21.

Table 1: Levels of independent variables in 3^2 factorial designs

Coded values Level	Independent variable values	
	Soy lecithin (X_1)	Ethanol (X_2)
-1	2	20
0	3	35
+1	5	50

CHARACTERIZATION OF SULFASALAZINE-LOADED ETHOSOMES

Particle size distribution and polydispersity index

The Malvern Zetasizer was used to determine the particle size distribution and polydispersity index of ethosomes at 25°C. A polystyrene cuvette held the samples (1 ml), and the measurements were recorded [25].

Zeta potential

A Malvern Zetasizer was used to measure the ethosomes' zeta potential at 25 °C. 1ml samples were placed within a polystyrene cuvette, and a zeta dip cell was used to determine the zeta potential [25].

Entrapment efficiency

In a centrifuge tube containing 1 mL of the sample, the formulation was centrifuged at 10,000 rpm for 1 h at 4°C. The amount of ethosomal formulation was measured using ultraviolet spectroscopy at 359 nm after the supernatant was collected. Entrapment efficiency was determined utilizing the subsequent equation [26].

$$EE\ (\%) = \frac{\textit{Amount of drug added during preparation} - \textit{Amount of free drug in the supernatant}}{\textit{Amount of drug added during preparation}} \times 100$$

Visualization by atomic force microscopy (AFM)

To evaluate the morphology of SE using AFM, a small water drop (approximately 10 microliters) of the formulation was applied to a silicon wafer and left to evaporate at room temperature. During AFM sample preparation, precautions were taken to minimize vesicle collapse by allowing the sample to dry slowly at room temperature without applying heat or forced airflow. This gentle drying method helps maintain the structural integrity of the ethosomal vesicles, which are soft and malleable. The images were observed using a multimode scanning probe microscope (Innova SPM, Bruker, Santa Barbara, CA) in semi-contact mode [27].

FTIR Spectroscopy

FT-IR analysis was performed with a JASCO FTIR 460 plus Fourier Transform spectrometer, scanning from 4000 to 400 cm^{-1}. Samples of the drug, excipients, physical mixture, and formulation were measured, suspended in KBr, and compressed into discs. These discs were analyzed with a resolution of 2 cm^{-1} [28].

Preparation of SE Gel

The ethosomal and conventional gels of Sulfasalazine were formulated by incorporating the optimized ethosomal suspension and pure drug into the 1% carbopol 934 gel. The conventional gel (CGL) was prepared by dispersing pure sulfasalazine (50 mg) into a 1% w/w Carbopol 934 gel base without any vesicular carriers. The Carbopol dispersion was neutralized with triethanolamine to obtain the required gel consistency. This ensured that the CGL served as a true control formulation containing only the drug and gel base, allowing fair and scientifically valid comparison with the ethosomal gel (EGL). 1g of carbopol was dissolved in 100 ml of distilled water and stirred for 2 hours before being allowed to swell overnight. Ethosomal suspension (equivalent to 50 mg of the drug) and 50 mg of the drug were separately introduced into 10 g of 1% carbopol 934 gel to obtain 1% ethosomal gel and 1% conventional gel, respectively. Continuous stirring was maintained during the introduction of triethanolamine to achieve the desired skin pH [29].

EVALUATION OF GEL INCORPORATED WITH SULFASALAZINE ETHOSOMES

Visual appearance

The ethosomal gels were visually inspected for uniformity, texture, absence of phase separation, and signs of aggregation [30].

Measurements of pH: Here, 20 ml of distilled water was used to dilute 1g of ethosomal gel to a rough weight. Next, the prepared gel solution was immersed, or the pH meter was placed in it. Three runs of the experiment were performed, and the average value was determined [31].

Drug content

Entrapment Efficiency (EE%) represents the percentage of sulfasalazine encapsulated within the ethosomal vesicles before they are incorporated into the gel. In contrast, Drug Content refers to the actual amount of sulfasalazine present in the final gel formulation after ethosomes have been added to the Carbopol base. Therefore, EE% evaluates vesicle loading efficiency, whereas Drug Content assesses the uniformity and accuracy of drug incorporation in the final gel. 0.5 g of the mixture was used, diluted in 10 ml of ethanol, and then filtered. With phosphate buffer, the volume was restored. Add phosphate buffer to bring the total to 10 ml after withdrawing 1 ml of the above solution. Thus, absorbance was determined using a UV-visible spectrophotometer at 359 nm [32].

Spreadability measurements

The assessment of spreadability is an essential phase in determining the appropriate viscosity and uniform spreading of gels. In practice, 1 g of the prepared gel was sandwiched between two glass slides of equal thickness (25 in.). After covering the slides with a 1kg weight for a minute, the gel was spread out across the slides. After the weight was finally removed, the spread area's diameter in (cm) was calculated [31].

Determination of viscosity

Viscosity of the prepared gel formulations was determined using a Brookfield viscometer (DV-II+; Brookfield Engineering

Laboratories, Middleboro, MA, USA) fitted with an SC4-18 spindle. The sample was maintained at a constant temperature of 25 ± 1°C, and the spindle was fully immersed in the gel during measurement. The spindle was rotated at a predetermined speed, and the sample's rotational resistance caused the instrument's calibrated spring to deflect. The viscosity of the formulation was then automatically calculated by the viscometer from the measured torque. The obtained viscosity values are shown in Figure 2 [33].

In-vitro drug release and kinetics of ethosomal gel

The Franz diffusion cell was used to conduct in vitro drug release studies. The donor compartment has two open ends, one of which has the diffusion membrane covered after being soaked in pH 7.4 phosphate buffer. 50mg of gel (equivalent to 2mg of the drug) was applied to the diffusion membrane. The receptor compartment was kept at 37±0.5ºC and contained 7.5 ml of pH 7.4 phosphate buffer agitated at 50 rpm. To maintain stable sink conditions, samples were collected at regular intervals for up to 12 hours and replaced with a fresh buffer solution. Ethosomal gel content in the receptor chamber was measured using a UV spectrophotometer at 359nm. Cumulative percentage of ethosomal gel permeation per unit area was plotted against time, facilitating flux value calculations from the slope [34]. Various kinetic models (Higuchi, first-order, Korsmeyer-Peppas, and Hixson-Crowell) were used to analyze drug release kinetics. The best-fit model, chosen based on the highest regression values among the formulations, was used to evaluate the in vitro release kinetics of the optimized formulations.

Ex vivo permeation studies

Goat ear skin was selected as the ex vivo model because its thickness, lipid composition, and follicular structure closely resemble human skin, making it a widely accepted substitute for percutaneous permeation studies. Freshly excised goat ear skin was carefully trimmed to remove hair and subcutaneous tissue to ensure uniform permeability. Using clean, hair-free skin minimizes barrier variability and yields accurate, reproducible permeation data when comparing the ethosomal gel with the conventional gel. In vitro experiments on skin permeation were conducted using goat ear skin via a Franz diffusion cell. The skin, obtained from a slaughterhouse, was soaked in phosphate buffer solution at pH 7.4 before mounting. The subcutaneous layer of the skin was positioned in the receptor compartment of the Franz diffusion cell, with its epidermal side facing the donor compartment. Gel formulations weighing 50 mg (equivalent to 2 mg of drug) were applied to the dermal side within the donor compartment. The receptor compartment contained 7.5 mL of pH 7.4 phosphate buffer, agitated at 50 rpm to ensure uniform mixing, and maintained at 37 ± 0.5 ºC. Sampling occurred at regular intervals up to 12 hours, with each withdrawn aliquot replaced by fresh buffer to maintain sink conditions. Drug content in the receptor chamber was quantified using a UV spectrophotometer at 359 nm. The cumulative percentage permeated per unit area was plotted against time, and flux was calculated from the slope [35].

In-vivo anti-inflammatory activity

The carrageenan model of paw edema was used to assess the anti-inflammatory efficacy of the test formulations in rats. The three groups of rats, with nine rats in each group. By injecting 0.1 ml of 0.1% w/v carrageenan into the plantar surface of the hind paw of those rats, an inflammation was induced, as shown in Figures 3 and 4. After carrageenan injection, test formulations, namely CGL and EGL gels, were applied topically to the injection site by friction at a dose of 100 mg. The paw volume was recorded at 0 h (just before), 1 h, and 3 h after test compound administration to the inflamed paw. The paw volume at the 0 h time point was nearly the same across all groups and was not statistically significant. At 1 h and 3 h, paw volume decreased significantly in the test formulations compared with the disease control, indicating anti-inflammatory activity [36].

Figure 3: Subplantar injection of Carrageenan to induce paw inflammation.

Figure 4: Inflamed area post carrageenan injection.

Statistical Analysis

All statistical analyses were performed using appropriate parametric tests. One-way ANOVA was used to compare multiple formulations for vesicle size, polydispersity index (PDI), zeta potential, entrapment efficiency, in vitro drug release, and ex vivo permeation parameters. When ANOVA results showed significance, Tukey's post-hoc test was applied to determine pairwise differences. Student's t-test was used for comparisons between two groups when applicable. A P-value < 0.05 was considered statistically significant. All analyses were conducted using Minitab software.

Table 2: Formulation of Sulfasalazine-loaded ethosomes applying 3^2 factorial designs

Batch code	Drug (mg)	Independent Variables		Dependent Variables			
		Soya lecithin (mg) X_1	Ethanol (ml) X_2	Particle size (nm)Y_1	Entrapment efficiency (%)Y_2	Zeta potential (mV)Y_3	Polydispersity Index (PDI)
SE1	50	2	20	110.7±1.53	85.33±3.84	-30.4±1.44	0.298 ± 0.02
SE2	50	2	35	143.5±2.51	86.05±1.62	-25.6±2.71	0.332 ± 0.03
SE3	50	2	50	187.7±3.12	88.65±2.15	-24.2±2.56	0.372 ± 0.02
SE4	50	3	20	103.8±1.49	87.31±2.43	-31.8±1.97	0.264 ± 0.01
SE5	50	3	35	139.0±1.38	89.23±2.89	-28.7±2.65	0.301 ± 0.02
SE6	50	3	50	169.6±1.59	90.51±2.21	-24.4±3.74	0.358 ± 0.02
SE7	50	5	20	98.3±2.37	91.96±1.67	-32.6±1.35	0.241 ± 0.02
SE8	50	5	35	106.0±1.76	94.62±1.34	-29.5±1.57	0.234 ± 0.01
SE9	50	5	50	127.9±2.15	92.46±3.46	-26.8±2.31	0.287 ± 0.02

RESULTS AND DISCUSSION

Formulation Design

In formulating ethosomes, we utilized an optimal 3^2-full-factorial design, maintaining Soya lecithin and Ethanol at X1 and X2 levels, respectively. Parameters p.s, z.p, and %EE, denoted as Y1, Y2, and Y3, were identified. Formulations were then optimized based on these input results [37]. Table 2 illustrates the response obtained from the factorial design.

Particle Size

This study examines the influence of solvent, surfactant (soy lecithin), and ethanol levels on ethosome particle size using Minitab factorial analysis. Particle size and Polydispersity Index (PDI) of sulfasalazine-loaded ethosomes were measured using a Malvern apparatus. Particle sizes ranged from 98.3±2.37 nm to 187.7±3.12 nm, and the particle size distribution graph is depicted in Table 2 and Figure 5, with PDI consistently < 1, indicating uniformity. A positive coefficient, like Ethanol, suggests that an increase in the corresponding factor leads to an increase in particle size. In contrast, a negative coefficient, like Soya Lecithin, indicates that an increase in that factor leads to a decrease in particle size. The magnitude of the coefficient indicates the strength of each factor's effect on particle size. Larger coefficients imply a greater impact on particle size. These findings emphasize the crucial role of formulation parameters in tailoring ethosome properties to optimize the efficacy of transdermal drug delivery. Particle size was plotted against Soya lecithin and Ethanol in Figure 6 [38].

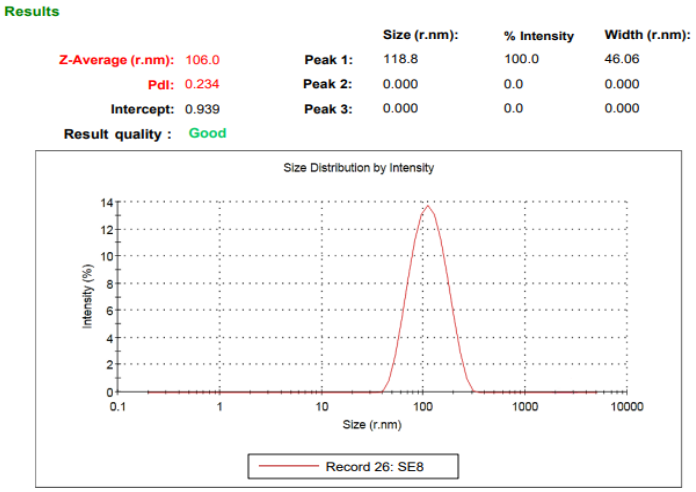

Figure 5: Particle size graph of SE8.

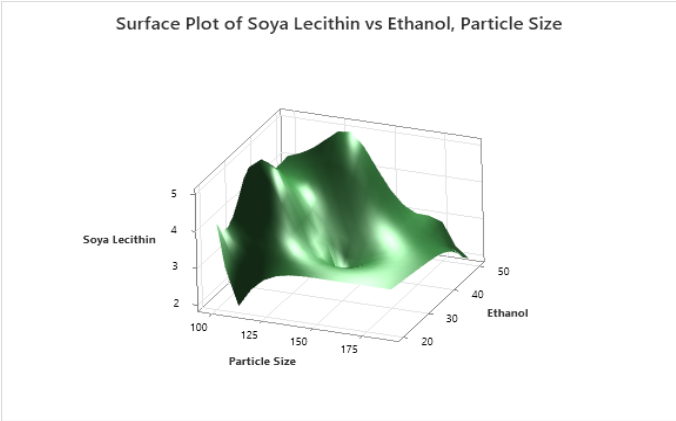

Figure 6: 3D Surface plot of particle size against Soya lecithin and Ethanol.

Regression Equation

Particle Size =131.83 + 15.47 Soya Lecithin_2 + 5.63 Soya Lecithin_3 - 21.10 Soya Lecithin_5 - 27.57 Ethanol_20 - 2.33 Ethanol_35 + 29.90 Ethanol_50.

Zeta Potential

Zeta potential plays a crucial role in determining vesicular properties such as vesicle–skin interaction and colloidal stability. The zeta potential of the ethosomal formulations was analyzed using a Minitab factorial design to evaluate the influence of Soya lecithin and ethanol concentrations on the stability of the vesicular system. The zeta potential values ranged from –24.2 ± 2.56 mV to –32.6 ± 1.35 mV, and the corresponding distribution graphs are presented in Table 2 and Figure 7. Generally, zeta potential values greater than ±30 mV are considered the stability threshold required to prevent vesicle aggregation. Since the ethosomal formulations in this study exhibited zeta potentials close to or exceeding this limit, the vesicular systems demonstrate acceptable electrostatic stability. Soya lecithin is a mixture of phospholipids, predominantly phosphatidylcholine, derived from soybeans and responsible for vesicle formation. In the factorial design model, Soya lecithin was evaluated at different levels (SL_2, SL_3, and SL_5), while ethanol concentrations were evaluated at Ethanol_20, Ethanol_35, and Ethanol_50. The statistical model indicates that increasing SL_2 decreases the zeta potential, that SL_3 slightly increases it, and that SL_5 significantly increases the zeta potential magnitude. Similarly, Ethanol_20 increases the zeta potential significantly, Ethanol_35 shows minimal effect, while Ethanol_50 reduces the zeta potential notably.

The negative surface charge of ethosomes is mainly attributed to the presence of ethanol in the formulation. Ethanol interacts with the polar phosphatidylcholine head groups of the phospholipids, disrupting hydrogen bonding and reducing lipid packing within the bilayer membrane. This interaction increases membrane fluidity and promotes greater exposure of negatively charged phosphate groups on the vesicle surface, resulting in increased electrostatic repulsion between vesicles. Additionally, increasing the concentration of soya lecithin increases the number of phospholipid molecules within the vesicular system, thereby enhancing the surface charge density & strengthening inter-vesicular repulsion. This effect minimizes vesicle aggregation and improves the colloidal stability of the ethosomal formulation. The surface plot illustrating the combined effect of Soya lecithin and ethanol on ZP is presented in Figure 8 [39].

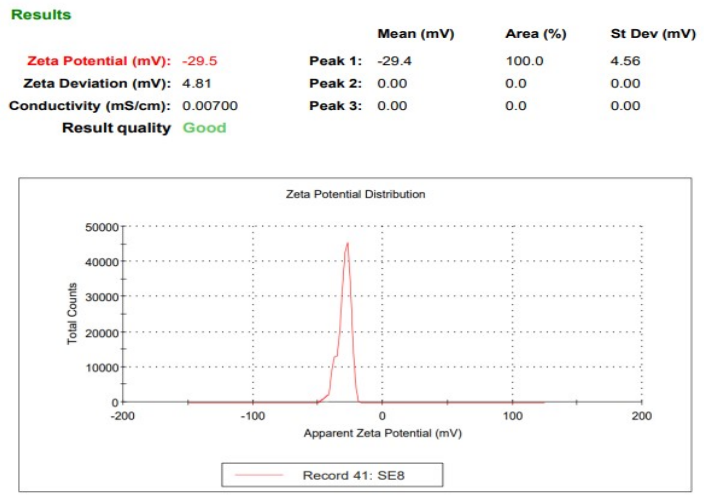

Figure 7: Zeta potential graph of SE8.

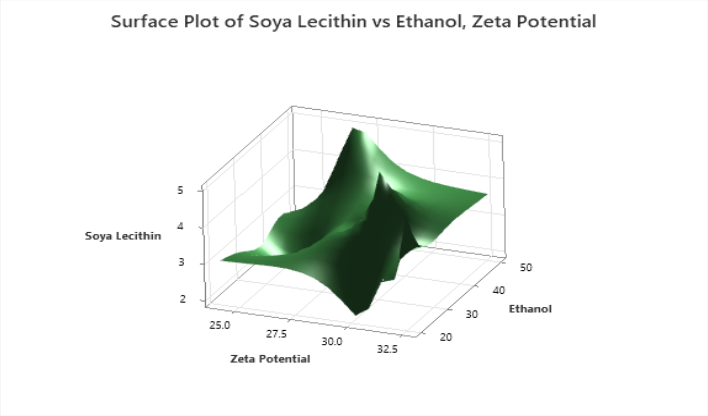

Figure 8: 3D Surface plot of Zeta Potential against Soya Lecithin and Ethanol.

Regression Equation

Zeta Potential = 28.222 - 1.489 Soya Lecithin_2 + 0.078 Soya Lecithin_3 + 1.411 Soya Lecithin_5 + 3.378 Ethanol_20 - 0.289 Ethanol_35 - 3.089 Ethanol_50.

Entrapment Efficiency

The entrapment efficiency of sulfasalazine-loaded ethosomes ranged from 85.33±3.84% to 94.62±1.34% and was directly correlated with Soya lecithin and Ethanol levels. Entrapment efficiency was notably influenced by SPC concentrations ranging from 2 to 5mg and ethanol concentrations ranging from 20 to 50 mL. Higher Soya Lecithin_2 reduces entrapment efficiency; Soya Lecithin_3 has a minor negative effect, whereas Soya Lecithin_5 significantly improves it. Increasing Ethanol_20 reduces the efficiency of the entrapped payload, Ethanol_35 has a minor positive effect, and Ethanol_50 significantly enhances efficiency. SE8 formulation, with 5mg surfactant and 35ml solvent, showed superior efficiency. These findings highlight the crucial importance of adjusting Soya

lecithin and Ethanol concentrations to enhance drug solubilization and optimize ethosome performance, as demonstrated in Table 2 and Figure 9, the surface plot of entrapment efficiency against Soya lecithin and Ethanol by using Minitab [38].

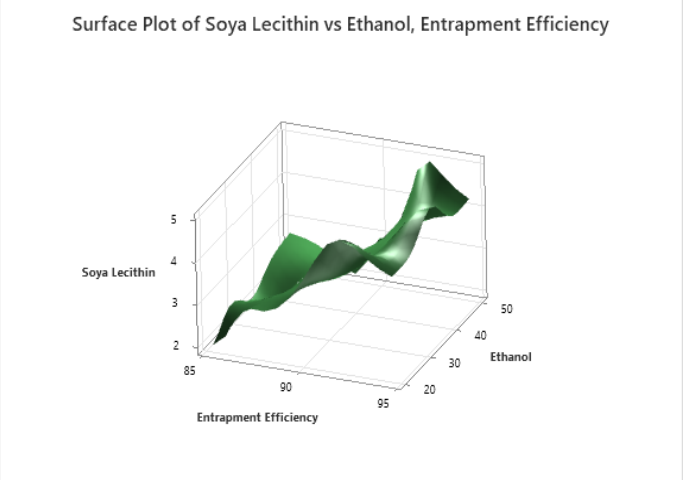

Figure 9: 3D Surface plot of Entrapment Efficiency against Soya Lecithin and Ethanol.

Regression Equation

Entrapment Efficiency = 89.569 - 2.892 Soya Lecithin_2 - 0.552 Soya Lecithin_3 + 3.444 Soya Lecithin_5 - 1.369 Ethanol_20 + 0.398 Ethanol_35 + 0.971 Ethanol_50

Fourier Transform Infra-red (FT-IR) Spectroscopy

FTIR analysis revealed peaks in sulfasalazine at 3061.44 cm-1 (OH), 1633.41 cm-1 (NH), and 1358.6 cm-1 (O=S=O). Soya lecithin exhibited peaks at 2932.23 cm-1 (C-H), 1633.48cm-1 (C=C), and 1744.3 cm-1 (C=O), while Cholesterol showed peaks at 3387.35 cm-1 (O-H), 2935.13 cm-1 (CH2), and 1673.91 cm-1 (C=C) functional groups, respectively. The principal peaks of Sulfasalazine were detected in both the physical mixture and the SE8 formulation spectra, indicating the absence of interaction between the drug and the excipients in the formulation [24]. Figure 10 represents the infrared spectra and Spectral interpretation of Sulfasalazine, Soya lecithin, Cholesterol, Physical mixture, optimized formulation (SE8).

Ethosomal Morphology

The particle size of the ethosomal formulation (SE8), as measured by AFM, was 116 nm. Topographic AFM images confirmed spherical shape with smooth surfaces, indicating stable morphology. The optimized formulation (SE8) is shown in Figure 11 [40].

Formulation and Characterization of Ethosomal Gel Incorporated with Sulfasalazine

Visual appearance of gel

The developed ethosomal gel exhibited excellent uniformity, smooth texture, and a translucent appearance. Its tactile sensation was slippery, and there were no discernible lumps, indicating even distribution of the ethosomal suspension within the carbopol gel [41].

Measurement of pH

The pH of Ethosomal gel formulations ranged from 6.1±0.15 to 6.8±0.05, aligning with the pH of human skin. Absence of skin irritation signs upon application of a gel. These values were sufficient to achieve good viscosity and clarity in the gels [42].

Drug content

The analysis of the prepared ethosomal gels indicated a drug content percentage ranging from 86.57±0.01% to 91.78±0.02%. These results signify minimal drug loss occurring during the gelling process [43].

Spreadability

Attaining the ideal properties of the prepared ethosomal gel depends on achieving favorable spreadability. Spreadability values not only mirror the gel's application behavior but also impact its therapeutic efficacy. The measured spreadability values for the SE8 ethosomal gel (1% Carbopol) were (12.5±0.17g cm/sec), indicating that Carbopol facilitates the formulation of easily spreadable ethosomal gel with low shearing force. These results suggest effortless application and prolonged site contact without leakage, ensuring enhanced therapeutic outcomes [44].

Rheological behavior of the prepared gel

Viscosity measurements were performed to determine the consistency of the ethosomal gel formulations, which is crucial for mucoadhesion & controlled drug release. The optimized ethosomal gel prepared using 1% Carbopol (SE8) exhibited a viscosity of 340.8 ± 0.21 cps. The concentration of Carbopol directly influenced viscosity, with higher polymer levels producing thicker gels due to increased cross-linking within the polymer network. The rheograms demonstrated shear-thinning behavior, facilitating easy application and preventing drainage from the site of application. Furthermore, the gel exhibited thixotropic properties, ensuring improved spreadability and rapid recovery of viscosity upon removal of shear stress, thereby

enhancing patient compliance. These rheological characteristics are important for pharmaceutical gel formulations & support effective drug delivery in a user-friendly manner [45]. The rheological behavior of the optimized ethosomal gel was further confirmed by the rheogram, which demonstrated a decrease in viscosity with increasing shear rate, indicating typical shear-thinning behavior, as shown in Figure 12.

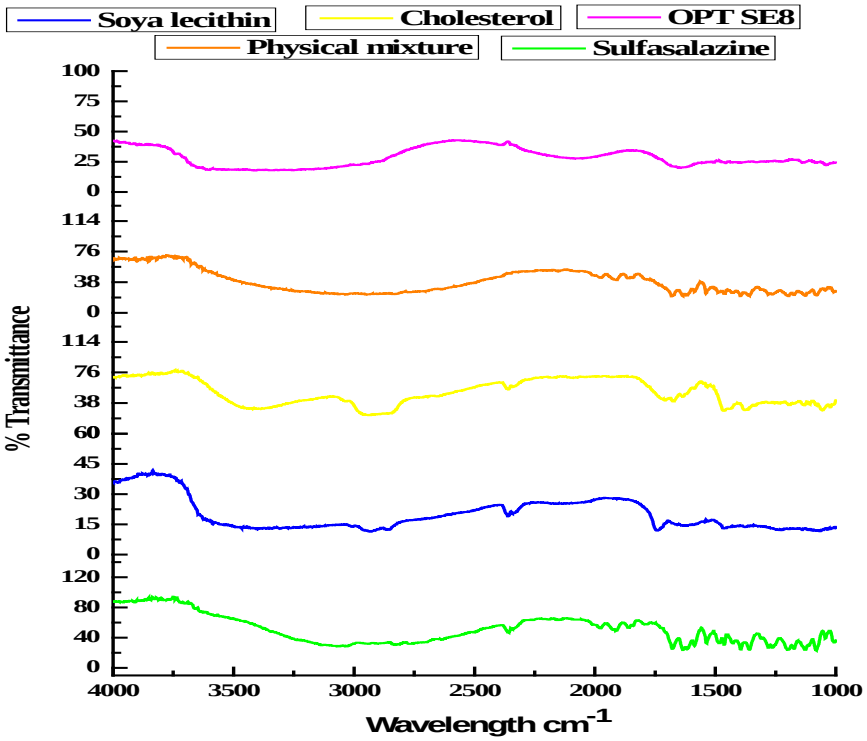

Figure 10: FT-IR graph of Sulfasalazine, Soya lecithin, Cholesterol, Physical mixture, optimized formulation (SE8).

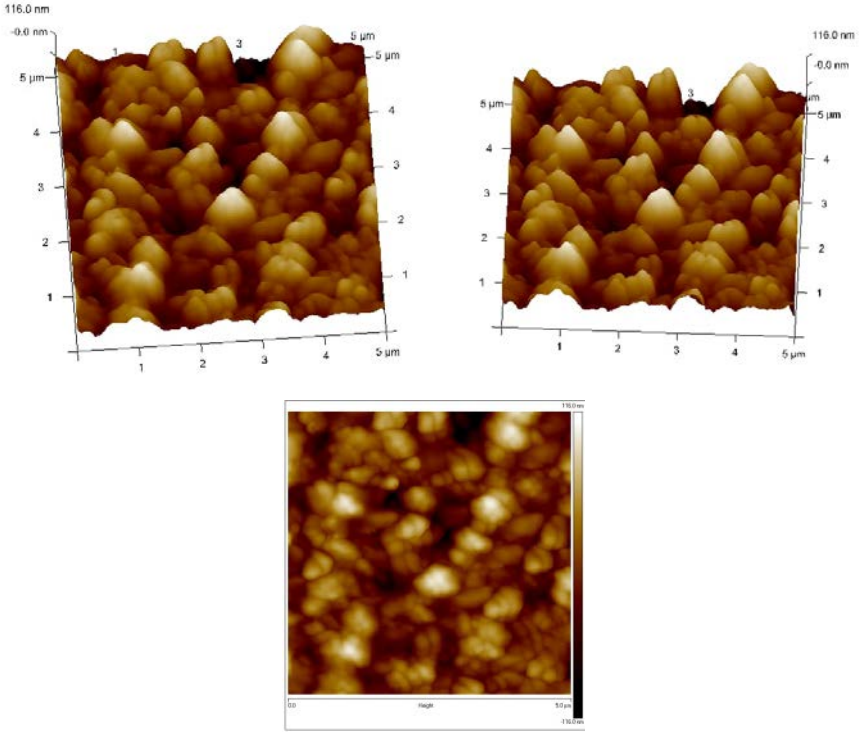

Figure 11: AFM image of the optimized formulation (SE8).

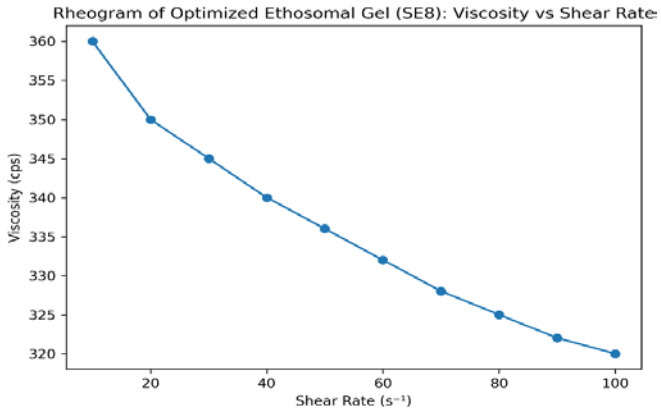

Figure 12: Rheogram of optimized ethosomal gel (SE8) showing viscosity as a function of shear rate, indicating shear-thinning behavior.

In-vitro Release

The release of Sulfasalazine from developed ethosomal gels was observed for up to 12 hours using the FDC method with a dialysis membrane. Drug diffusion across the ethosomal gels is the mechanism of drug release. Upon analyzing the drug-release patterns of all nine formulations over 12 hours, it was determined that SE8 exhibited superior drug release compared with the other formulations. Consequently, SE8 was selected as the final formulation, achieving an 83.31% release rate. This controlled release for the entire 12-hour duration was attributed to the effective entrapment of the drug within the ethosomal gel. It was observed that the structure and characteristics of the lipids played a crucial role in controlling the drug release. The release profile of all 9 formulations is depicted in Figure 13. Various kinetic models, including the Higuchi, first-order, Korsmeyer-Peppas, and Hixson-Crowell models, were employed. Notably, for formulation SE8, the Korsmeyer-Peppas model exhibited the most favorable fit, displaying an almost linear plot with the highest R2 value. This observation indicates that diffusion primarily governs drug release. The release kinetics of SE8 in various models are depicted in Table 3 [46].

Table 3: Different release kinetics of SE8.

Formulation	Models				
	Zero Order	First Order	Higuchi	Korsmeyer-Peppas	Hixson-Crowell
SE8	0.9788	0.9152	0.8079	0.9933	0.9375

***In-vitro* Drug release profile**

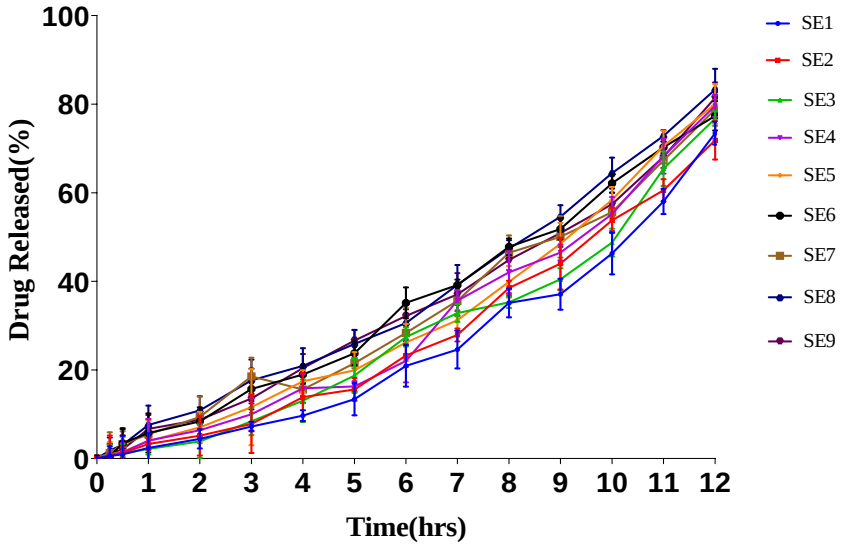

Figure 13: % Cumulative drug release profiles of SE1 to SE9.

Ex Vivo Diffusion Study of Sulfasalazine Ethosomal Gel

The permeation profile of the drug from goat ear skin is a pivotal factor in evaluating the efficacy of drug delivery systems. In this study, the permeation of Sulfasalazine through the goat ear skin was compared between a selected formulation (SE8) and a conventional gel (CGL). Remarkably, the final formulation exhibited a significant enhancement, with 66.81% of the drug permeating from the Sulfasalazine-loaded ethosomal gel over 12 hours, compared to 37.48% for CGL. This enhanced permeation is likely due to ethanol in the EGL core, which aids lipid solubilization in the stratum corneum and facilitates vesicle penetration. Figure 14 illustrates the amount of Sulfasala- zine permeated from the finalized formulation (SE8) compared to CGL to the model group ($P < 0.009$). The presence of ethanol in

ethosomes may effectively dissolve skin lipids, potentially overcoming skin barriers for efficient drug delivery [47].

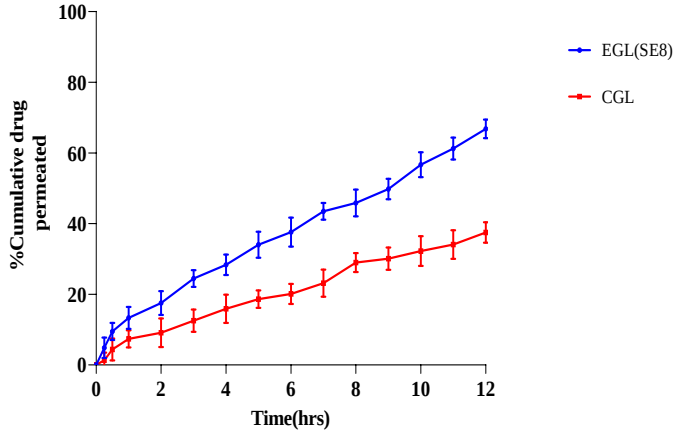

Figure 14: Percentage of drug permeation from conventional gel and ethosomal gel (SE8).

In vivo anti-inflammatory activity

The paw volume was measured after application of the test formulations at 0 h (immediately after treatment), 1 h, and 3 h post-treatment, as shown in Figures 15-17.

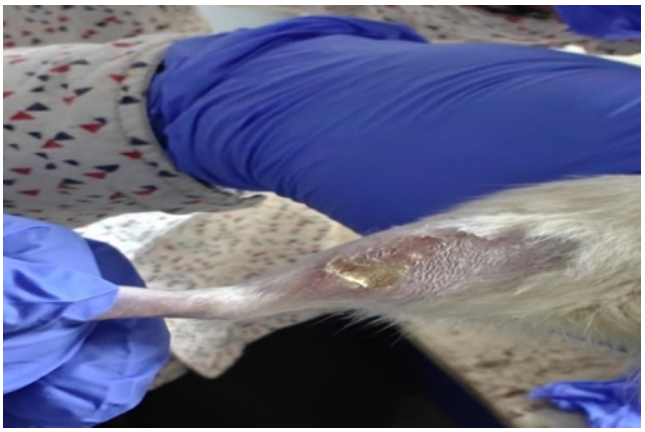

Figure 15: Application of EGL

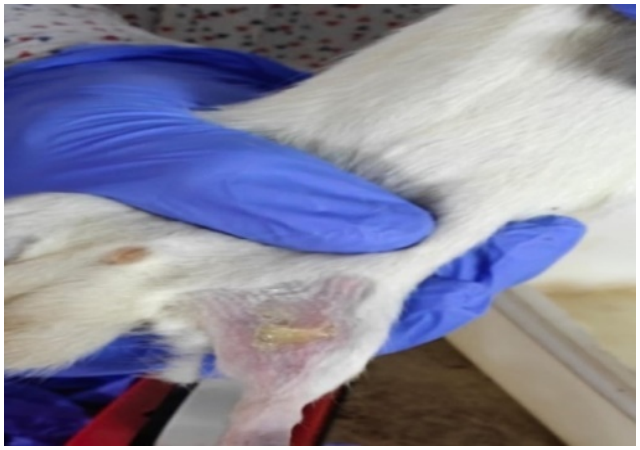

Figure 16: Application of CGL

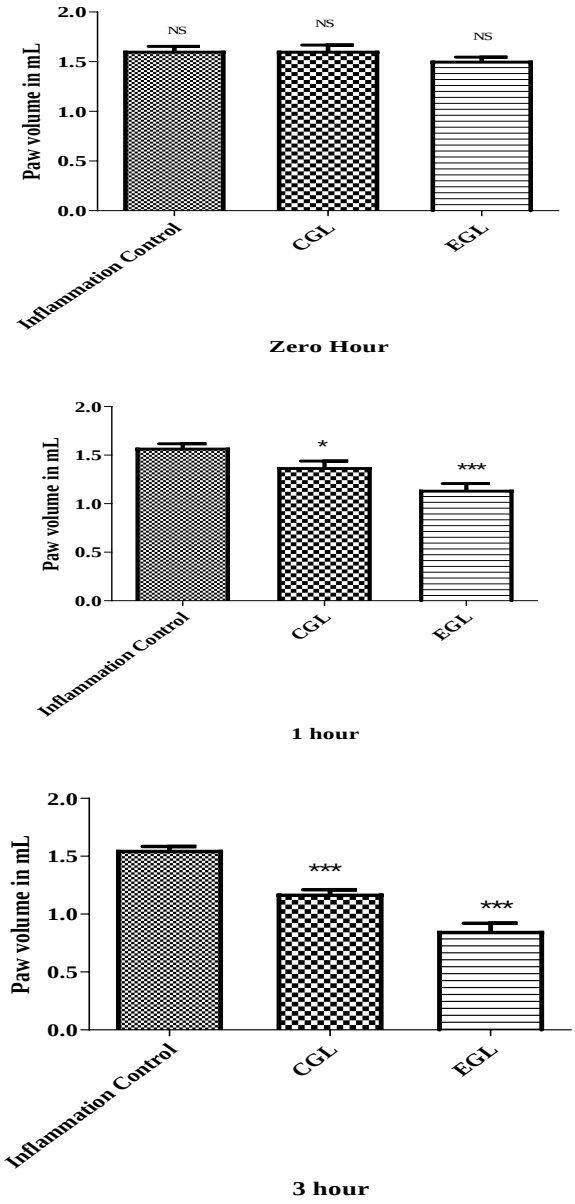

Figure 17: Paw volume measurement at different time-points across the groups.

The paw volume at 0 h was similar across all the groups. At 1 h and 3 h, paw volume decreased significantly in the test formulations compared to the disease control, indicating strong anti-inflammatory activity, with the effect peaking and persisting until 3 h. However, the overall efficacy of the EGL was most potent, followed by CGL, as indicated by statistical analysis of the model group (***P < 0.001). Thus, it can be concluded that both test formulations, EGL and CGL, are beneficial in the treatment of inflammatory conditions in SD rats for long durations under the given experimental conditions, with EGL being more potent than CGL [36].

The anti-inflammatory activity was evaluated for 3 hrs because the carrageenan-induced paw edema model is an acute inflammatory model in which the inflammatory response peaks within 1–3 hours and then naturally subsides. Therefore, this model is not suitable for extended observation periods such as 6, 12, or 24 hours. Although in vivo evaluation could not be extended beyond 3 hours for this reason, the sustained behavior of the ethosomal gel was demonstrated through 12-hour in vitro release and ex vivo permeation studies. Future work will include long-duration pharmacodynamic models or chronic inflammation studies to further validate the formulation's sustained anti-inflammatory potential.

CONCLUSION

The developed ethosomal gel presents a promising strategy for the transdermal delivery of Sulfasalazine to treat rheumatoid arthritis. Through systematic formulation optimization and comprehensive characterization, including AFM analysis, the particle sizes ranged from 98.3 ± 2.37 nm to 187.7 ± 3.12 nm, with negative zeta potential values between –24.2 ± 2.56 mV and –32.6 ± 1.35 mV, while the entrapment efficiency ranged from 85.33 ± 3.84% to 94.62 ± 1.34%. The ethosomal gel exhibited favorable physicochemical properties for effective drug delivery. The incorporation of Sulfasalazine-loaded ethosomes into a Carbopol gel facilitated controlled drug release for up to 12 hours, with the optimized formulation exhibiting 83.31 ± 0.01% drug release.

The ex vivo permeation study demonstrated that the ethosomal gel (EGL) exhibited higher permeability (66.81 ± 0.02%) than the conventional gel (CGL) (37.48 ± 0.10%). Furthermore, both EGL and CGL demonstrated beneficial anti-inflammatory activity in SD rats under the given experimental conditions, with EGL showing greater potency than CGL. These findings highlight the potential of the ethosomal gel as a promising transdermal delivery system for Sulfasalazine, which may help overcome certain limitations associated with oral administration while offering enhanced drug release and improved anti-inflammatory efficacy. Thus, this study provides valuable insights into the development of transdermal drug delivery systems for localized treatment of rheumatoid arthritis. In the present study, the primary objective was to evaluate the transdermal delivery potential of the developed Sulfasalazine-loaded ethosomal gel through formulation optimization, physicochemical characterization, ex vivo permeation, and in vivo anti-inflammatory evaluation. A direct comparison with an oral control group was not included in the current experimental design. Therefore, the conclusion statement has been revised to avoid overstatement and to clarify that the developed formulation may help overcome certain limitations associated with oral administration.

FINANCIAL ASSISTANCE

NIL

CONFLICT OF INTEREST

The authors declare no conflict of interest.

AUTHOR CONTRIBUTION

Sanjaikumar D. conceptualized the research idea, designed the study plan, and led the investigation and execution of the experimental work. He was primarily responsible for data collection, analysis, visualization, and the preparation of the original manuscript draft. Anasuya Patil provided continuous supervision throughout the project, ensured the overall quality of the research, and contributed to the review and refinement of the manuscript. Hemanth G. offered critical support in software handling and validation of key data outputs. All authors contributed to the interpretation of results, reviewed the final manuscript, and approved it for publication.

DECLARATION OF USE OF AI TOOLS

The authors used ChatGPT (OpenAI) solely to assist with language editing, grammar correction, and improving the readability of the manuscript. The AI tool was not used to generate, analyze, or interpret experimental data or to draw scientific conclusions. All scientific content, results, interpretations, and conclusions were independently reviewed and verified by the authors. The authors take full responsibility for the originality, accuracy, and integrity of this manuscript.

REFERENCES

[1] Di Matteo A, Bathon JM, Emery P. Rheumatoid arthritis. *Lancet*, **402**(10416), 2019–2033 (2023) https://doi.org/10.1016/S0140-6736(23)01525-8

[2] Radu AF, Bungau SG. Management of rheumatoid arthritis: an overview. *Cells*, **10**(11), 2857 (2021) https://doi.org/10.3390/cells10112857

[3] Chabib L, Ikawati Z, Martien R, Ismail H, Wahyudi MDP, Arimurni DA, et al. Rheumatoid arthritis and the challenge of using nanoparticles for its treatment. *MATEC Web Conf*, **154**, 04005 (2018) https://doi.org/10.1051/matecconf/201815404005

[4] Chauhan N, Vasava P, Khan SL, Siddiqui FA, Islam F, Chopra H, et al. Ethosomes: a novel drug carrier. *Ann Med Surg (Lond)*, **82**, 104595 (2022) https://doi.org/10.1016/j.amsu.2022.104595

[5] Dik B, Sonmez G, Faki HE, Bahcivan E. Sulfasalazine treatment can cause a positive effect on LPS-induced endotoxic rats. *Exp Anim*, **67**(4), 403–412 (2018) https://doi.org/10.1538/expanim.18-0029

[6] Azizah N, Ghifari AA, Adikusuma W, Darmawi, Hamidy MY. Exploring the diverse therapeutic benefits of metformin: from anti-cancer to anti-inflammation and PCOS management. *J Appl Pharm Res*, **12**(4), 1–10 (2024) https://doi.org/10.69857/joapr.v12i4.573

[7] Soltani A, Erfani Moghadam V, Yahyazadeh A, Mahmoodi NO. Synthesis, spectroscopic characterization, molecular docking, and in vitro cytotoxicity of calcium(II) sulfasalazine complex. *J Mol Struct*, **1267**, 133568 (2022) https://doi.org/10.1016/j.molstruc.2022.133568

[8] Cai J, Mar JS, Kapili B, Storek KM, Uzunovic J, et al. Spatiotemporal characterization of sulfasalazine and 5-ASA pharmacokinetics using a noninvasive intestinal sampling device. *Clin Pharmacol Ther*, **118**(6), 1437–1442 (2025) https://doi.org/10.1002/cpt.70035

[9] Muteeb G, Rehman MT, Shahwan M, Aatif M. Origin of antibiotics and antibiotic resistance, and their impacts on drug development: a narrative review. *Pharmaceuticals*, **16**(11), 1615 (2023) https://doi.org/10.3390/ph16111615

[10] Dolinger M, Torres J, Vermeire S. Crohn's disease. *Lancet*, **403**(10432), 1177–1191 (2024) https://doi.org/10.1016/S0140-6736(23)02586-2

[11] Huang S, Cheemarla VKR, Tiana D, Lawrence SE. Exploring the crystal structure landscape of sulfasalazine through various multicomponent crystals. *Cryst Growth Des*, **23**(8), 5446–5461 (2023) https://doi.org/10.1021/acs.cgd.2c01403

[12] Anwar DM, Khattab SN, Helmy MW, Kamal MK, Bekhit AA, Elkhodairy KA, et al. Lactobionic/folate dual-targeted amphiphilic maltodextrin-based micelles for targeted codelivery of sulfasalazine and resveratrol to hepatocellular carcinoma. *Bioconjug Chem*, **29**(9), 3026–3041 (2018) https://doi.org/10.1021/acs.bioconjchem.8b00428

[13] Zeng T, Ye JZ, Qin H, Xu QQ. Systematic review and network meta-analysis of different non-steroidal anti-inflammatory drugs for juvenile idiopathic arthritis. *World J Clin Cases*, **12**(12), 2056–2064 (2024) https://doi.org/10.12998/wjcc.v12.i12.2056

[14] Al Muqbil R, Aldhubiab B. Ethosome-based transdermal drug delivery: structural components, preparation techniques, and therapeutic applications across metabolic, chronic, and oncological conditions. *Pharmaceutics*, **17**(5), 583 (2025) https://doi.org/10.3390/pharmaceutics17050583

[15] Manpreet M, Sachdeva S, Kaur H, Garg R, Singh J. Ethosomes: a revolutionary approach in advanced drug delivery systems. *J Drug Deliv Ther*, **15**(2), 186–192 (2025) https://doi.org/10.22270/jddt.v15i2.6993

[16] Kumar S, Verma D, Yadav R, Singh S, Sharma P. In vitro release, ex vivo penetration, and in vivo dermatokinetics of ketoconazole loaded solid lipid nanoparticles for topical delivery. *Eur J Pharm Biopharm*, **158**, 152–164 (2021) https://doi.org/10.1016/j.ejpb.2020.11.009

[17] Ahsan MU, Ambreen U, Javed H, Noor N, Jan M, Khan MN. NSAID associated renal injury: mechanisms, risks, and safer strategies. *Arch Nephrol Ren Stud*, **5**(1), 1–5 (2025) https://doi.org/10.33696/nephrology.5.013

[18] Rancan F. Drug delivery to skin by nanotechnology-based drug delivery systems. *J Pharm Drug Deliv Res*, **7**, 1–6 (2018) https://doi.org/10.4172/2325-9604.1000183

[19] Devaki J, Pavuluri S, Suma N. Ethosomes: a vesicular carrier as a novel tool for transdermal drug delivery system. *J Drug Deliv Ther*, **13**(4), 159–164 (2023) https://doi.org/10.22270/jddt.v13i4.5796

[20] Singh V, Chaubey N. Design and evaluation of topical hydrogel formulation of aceclofenac for improved therapy. *J Drug Deliv Ther*, **9**(5), 118–122 (2019) https://doi.org/10.22270/jddt.v9i5.3605

[21] El-Mahdy MM, Hassan AS, El-Badry M, El-Gindy GE. Performance of curcumin in nanosized carriers niosomes and ethosomes as potential anti-inflammatory delivery system for topical application. *Bull Pharm Sci Assiut*, **43**(1), 105–122 (2020) https://doi.org/10.21608/bfsa.2020.93599

[22] Digkas T, Tefas LR, Porfire AS, Tomuta I, De Beer T. Continuous manufacturing of a topical hydrogel with clobetasol propionate loaded liposomes using QbD methodology. *Int J Pharm*, **682**, 125964 (2025) https://doi.org/10.1016/j.ijpharm.2025.125964

[23] Wilson V, Siram K, Rajendran S, Sankar V. Development and evaluation of finasteride loaded ethosomes for targeting to the pilosebaceous unit. *Artif Cells Nanomed Biotechnol*, **46**(8), 1892–1901 (2018) https://doi.org/10.1080/21691401.2017.1396221

[24] Hajare A, Dol H, Patil K. Design and development of terbinafine hydrochloride ethosomal gel for enhancement of transdermal delivery: in vitro, in vivo, molecular docking, and stability study. *J Drug Deliv Sci Technol*, **61**, 102280 (2021) https://doi.org/10.1016/j.jddst.2020.102280

[25] Schreiner TB, Santamaria Echart A, Ribeiro A, Peres AM, Dias MM, Pinho SP, et al. Formulation and optimization of nanoemulsions using the natural surfactant saponin from Quillaja bark. *Molecules*, **25**(7), 1538 (2020) https://doi.org/10.3390/molecules25071538

[26] Shen G, Li Z, Wang J, Yang H, Zhang X. Enhanced transdermal delivery of apremilast loaded ethosomes: optimization, characterization and in vivo evaluation. *J Drug Deliv Sci*

Technol, **91**, 105211 (2024) https://doi.org/10.1016/j.jddst.2023.105211

[27] Dhas N, Preetha HS, Dubey A, Ravi G, Govindan I, Rama A, et al. Factorial design based fabrication of biopolymer functionalized Asiatic acid embedded liposomes: in vitro characterization and evaluation. *J Appl Pharm Sci*, **12**(11), 71–81 (2022) https://doi.org/10.7324/JAPS.2022.121108

[28] Mazzotta E, Marazioti A, Mourtas S, Muzzalupo R, Antimisiaris SG. Liposomes coated with novel synthetic bifunctional chitosan derivatives as potential carriers of anticancer drugs. *Pharmaceutics*, **16**(3), 319 (2024) https://doi.org/10.3390/pharmaceutics16030319

[29] Supraja R, Sailaja AK. Formulation of mefenamic acid loaded ethosomal gel by hot and cold methods. *Nano Biomed Eng*, **9**(1), 27–35 (2017) https://doi.org/10.5101/nbe.v9i1.p27-35

[30] Amarachinta PR, Sharma G, Samed N, Chettupalli AK, Alle M, Kim JC. Central composite design for the development of carvedilol loaded transdermal ethosomal hydrogel for extended and enhanced antihypertensive effect. *J Nanobiotechnol*, **19**, 100 (2021) https://doi.org/10.1186/s12951-021-00833-4

[31] Sakran W, Abdel Rashid RS, Saleh F, Abdel Monem R. Ethosomal gel for rectal transmucosal delivery of domperidone: design of experiment, in vitro, and in vivo evaluation. *Drug Deliv*, **29**(1), 1477–1491 (2022) https://doi.org/10.1080/10717544.2022.2072542

[32] Adepu S, Ramakrishna S. Controlled drug delivery systems: current status and future directions. *Molecules*, **26**(19), 5905 (2021) https://doi.org/10.3390/molecules26195905

[33] Harun SN, Nordin SA, Gani SSA, Shamsuddin AF, Basri M, Basri HB. Development of nanoemulsion for efficient brain parenteral delivery of cefuroxime: designs, characterizations, and pharmacokinetics. *Int J Nanomedicine*, **13**, 2571–2584 (2018) https://doi.org/10.2147/IJN.S151788

[34] Kumar J, Bhardwaj M, Bisht D, Bisht M. Advances in topical antiviral drug delivery: role of liposomes and nanotechnology based strategies. *J Neonatal Surg*, **14**(30S), 963–974 (2025) https://doi.org/10.63682/jns.v14i30S.7504

[35] Batur E, Özdemir S, Durgun ME, Özsoy Y. Vesicular drug delivery systems: promising approaches in ocular drug delivery. *Pharmaceuticals*, **17**(4), 511 (2024) https://doi.org/10.3390/ph17040511

[36] Chen JG, Liu YF, Gao TW. Preparation and anti-inflammatory activity of triptolide ethosomes in an erythema model. *J Liposome Res*, **20**(4), 297–303 (2010) https://doi.org/10.3109/08982100903544144

[37] Gupta M, Tiwari P. Formulation and in-vitro evaluation of oxaprozin transdermal patches for sustained anti-inflammatory therapy. *J Appl Pharm Res*, **13**(6), 22–32 (2025) https://doi.org/10.69857/joapr.v13i6.1203

[38] Al Ghoush WH, Al Baz AA, Al Bassam MA, Al Dulaimi TH, Al Hashimi AR. A DoE based development and characterization of Nadifloxacin loaded transethosomal gel for the treatment of acne vulgaris. *Future J Pharm Sci*, **10**, 46 (2024) https://doi.org/10.1186/s43094-024-00616-2

[39] Kang Y, Zhang S, Wang G, Yan Z, Wu G, Tang L, et al. Nanocarrier based transdermal drug delivery systems for dermatological therapy. *Pharmaceutics*, **16**(11), 1384 (2024) https://doi.org/10.3390/pharmaceutics16111384

[40] Emanet M, Ciofani G. Liposomes and ethosomes: comparative potential in enhancing skin permeability for therapeutic and cosmetic applications. *Cosmetics*, **11**(6), 191 (2024) https://doi.org/10.3390/cosmetics11060191

[41] Ismail TA, Shehata TM, Mohamed DI, Elsewedy HS, Soliman WE. Quality by design for development, optimization and characterization of brucine ethosomal gel for skin cancer delivery. *Molecules*, **26**(11), 3454 (2021) https://doi.org/10.3390/molecules26113454

[42] Yılmaz Usta D, Teksin ZS, Tugcu-Demiroz F. Evaluation of emulgel and nanostructured lipid carrier-based gel formulations for transdermal administration of ibuprofen: characterization, mechanical properties, and ex-vivo skin permeation. *AAPS PharmSciTech*, **25**, 124 (2024) https://doi.org/10.1208/s12249-024-02831-9

[43] Ansari SA, Qadir A, Warsi MH, Mujeeb M, Aqil M, Mir SR, et al. Ethosomes-based gel formulation of karanjin for treatment of acne vulgaris: in vitro investigations and preclinical assessment. *3 Biotech*, **11**(11), 456 (2021) https://doi.org/10.1007/s13205-021-02978-3

[44] Sanjana A, Ahmed MG, Gowda BHJ. Preparation and evaluation of in-situ gels containing hydrocortisone for the treatment of aphthous ulcer. *J Oral Biol Craniofac Res*, **11**(2), 269–276 (2021) https://doi.org/10.1016/j.jobcr.2021.02.001

[45] Daood NM, Jassim ZE, Ghareeb MM, Zeki H. Studying the effect of different gelling agents on the preparation and characterization of metronidazole as topical emulgel. *Asian J Pharm Clin Res*, **12**(3), 571–577 (2019) https://doi.org/10.22159/ajpcr.2019.v12i3.31504

[46] Anju K, Priya S, Sandeep DS, Nayak P, Kumar P, Kumar A, et al. Formulation and optimization of zaltoprofen loaded ethosomal gel by using 2^3 full factorial designs. *J Pharm Res Int*, **33**(24B), 30–44 (2021) https://doi.org/10.9734/jpri/2021/v33i24B31439

[47] Peram MR, Jalalpure SS, Kumbar VM, Patil SR, Joshi SA, Bhat KG, et al. Factorial design-based curcumin ethosomal nanocarriers for skin cancer delivery: in vitro evaluation. *J Liposome Res*, **29**(3), 291–311 (2019) https://doi.org/10.1080/08982104.2018.1556292